Systematic analysis of *bZIP* gene family in *Suaeda australis* reveal their roles under salt stress

Yinquan Qu[1†], Ji Wang[2†], Tianxiang Gao[1], Caihui Qu[1], Xiaoyun Mo[1] and Xiumei Zhang[1*]

Abstract

Background *Suaeda australis* is one of typical halophyte owing to high levels of salt tolerance. In addition, the *bZIP* gene family assumes pivotal functions in response to salt stress. However, there are little reports available regarding the *bZIP* gene family in *S. australis*.

Results In this study, we successfully screened 44 *bZIP* genes within *S. australis* genome. Subsequently, we conducted an extensive analysis, encompassing investigations into chromosome location, gene structure, phylogenetic relationship, promoter region, conserved motif, and gene expression profile. The 44 *bZIP* genes were categorized into 12 distinct groups, exhibiting an uneven distribution among the 9 chromosomes of *S. australis* chromosomes, but one member (*Sau23745*) was mapped on unanchored scaffolds. Examination of cis-regulatory elements revealed that bZIP promoters were closely related to anaerobic induction, transcription start, and light responsiveness. Comparative transcriptome analysis between ST1 and ST2 samples identified 2,434 DEGs, which were significantly enriched in some primary biological pathways related to salt response-regulating signaling based on GO and KEGG enrichment analysis. Expression patterns analyses clearly discovered the role of several differently expressed *SabZIPs*, including *Sau08107*, *Sau08911*, *Sau11415*, *Sau16575*, and *Sau19276*, which showed higher expression levels in higher salt concentration than low concentration and a response to salt stress. These expression patterns were corroborated through RT-qPCR analysis. The six differentially expressed *SabZIP* genes, all localized in the nucleus, exhibited positive regulation involved in the salt stress response. SabZIP14, SabZIP26, and SabZIP36 proteins could bind to the promoter region of downstream salt stress-related genes and activate their expressions.

Conclusions Our findings offer valuable insights into the evolutionary trajectory of the *bZIP* gene family in *S. australis* and shed light on their roles in responding to salt stress. In addition to fundamental genomic information, these results would serve as a foundational framework for future investigations into the regulation of salt stress responses in *S. australis*.

Keywords *Suaeda australis*, *bZIP* gene family, Expression patterns, Salt stress, Genomic

[†]Yinquan Qu and Ji Wang contributed equally to this work.

*Correspondence:
Xiumei Zhang
xiumei1227@163.com
[1] Fishery College, Zhejiang Ocean University, Zhoushan 316022, Zhejiang, China
[2] School of Teacher Education, Nanjing Xiaozhuang University, Nanjing 211171, Jiangsu, China

Background

Coastal wetlands play crucial roles in climate change mitigating, carbon sequestering, and biodiversity support [1, 2]. Unfortunately, over the past few decades, more than one-third of coastal wetlands have experienced a decline in their ecological functionality [3]. The presence of plants is crucial for the preservation of ecological function in coastal wetlands, particularly in terms of

Qu *et al. BMC Plant Biology*   (2024) 24:816

Page 2 of 17

enhancing biodiversity [4]. However, substantial variations in salinity levels within coastal wetlands can directly impair plant capabilities, leading to inhibited growth or, in severe cases, plant mortality [5].

Suaeda australis belonging to the genus *Suaeda* (Chenopodiaceae), is mainly distributed in the subtropical and tropical coastal areas of China, Japan and Oceanica [6]. Pharmacological studies showed that antioxidant and antibacterial activities were found in the extracts of *S. australis* leaves [7]. Owing to the high nutritional value, the leaves of *S. australis* have long been used as food ingredient and supplementary feed [8]. Especially, *S. australis* is a typical halophyte, which can improve the coastal marsh saline-alkali land, reduce pollutants, and protect the coastline [9]. However, the growth zone of *S. australis* gradually moved from intertidal zone with higher salt concentration to suprapatid zone with lower salt concentration, which is caused by extreme fluctuations in salinity in coastal wetlands. More severely, the amounts of *S. australis* of suprapatid zone had fallen sharply in the past decades. Hence, it is of great scientific significance and ecological value to investigate the salt tolerance mechanism of *S. australis* in depth for the conservation of *S. australis,* utilization of saline soil resources, improvement of coastal salt-alkali environment, and development of marine agricultural economy. The assembled genome size of *S. australis* was 437.17 Mb and 408.45 Mb (93.43%) of sequences were integrated into 9 pseudo-chromosomes with 24,371 annotated protein-coding genes.

Many valuable genes associated with stress responses need to be identified to enhance stress tolerance effectively for *S. australis*. As one of the greatest family encoding transcription factors (TFs), the basic leucine zipper (*bZIP*) gene family plays fundamental roles in environmental and developmental signalling as well as stress response in plants [10]. Previous studies reported that bZIP TFs play pivotal roles in salt stress response [11]. The bZIP TFs typically consist of 60–80 amino acids, containing a bZIP domain characterized by a highly conserved basic region and a variable leucine zipper region [12]. bZIP TFs were categorized into different subgroups based on conserved domains [13]. In addition, the *bZIP* genes involved in salinity stress varied among different plants. For example, the *OsbZIP12*, *OsbZIP72* and *OsbZIP46* genes confer stronger salt tolerant than other members in rice bZIP family [14], while *GmbZIP 62*, *GmbZIP44*, and *GmbZIP 78* genes of soybean are significantly upregulated in reaction to salt stress [15–17].

So far, little reports on the functional characterization of bZIP TFs are available. To identify potential *bZIP* genes involved in regulation of salt stress responses, this study systematically identified and characterized all *bZIP* genes in *S. australis*. We performed a detailed analysis of genome distribution, gene structure, and expression patterns in response to salt stress. Finally, we identified the candidate *bZIP* genes that exhibit potential responsiveness to salt stress through transcriptome analysis and quantitative real-time PCR (qRT-PCR) evaluation.

Results

Genome-wide identification of the *SabZIP* gene family in *S. australis*

SabZIP genes were identified in *S. australis* genome based on HMM program and the local BLASTP analyses. As a result, 44 identified *SabZIP* genes were serially named *SabZIP01* through *SabZIP44* for convenience (Supplementary Table S1). Additionally, it was observed that substantial variations existed among the *SabZIP* genes in terms of mRNA transcript length and the protein sequences they encoded. Additionally, the results indicated considerable diversity among *SabZIP* genes in terms of mRNA transcript lengths and the corresponding protein sequences. The mRNA products (CDS) of 44 *SabZIP* genes exhibited lengths spanning from 420 to 2352 bp, and the corresponding translated protein sequences displayed variations in amino acid counts ranging from 140 to 784. Among these sequences, *SabZIP23* featured the shortest amino acid sequence, comprising only 143 amino acid residues, whereas *SabZIP20* was characterized by the longest sequence, encompassing 784 amino acid residues. The theoretical isoelectric point (PI) values ranged from 4.91 (*SabZIP14*) and 9.69 (*SabZIP15*), and the molecular mass of bZIP members ranged from 16.12 (*SabZIP11*) to 86.06 kDa (*SabZIP20*) (Supplementary Table S1).

Chromosome location and synteny analysis of *SabZIP* genes

Except for *SabZIP44*, all *SabZIP* genes in *S. australis* were mapped onto nine chromosomes (Chrs), as illustrated in Fig. 1. The highest count of *SabZIP* genes per chromosome was observed on Chr8, where nine *SabZIP* genes were located. Seven genes per chromosome were located on Chr3 and Chr6; five were found on Chr5, Chr7, and Chr9; two genes each were located on Chr2 and Chr4. Chr1 and Scaffold_136 contained the lowest counts of *SabZIP* genes, with only one each. For genome mining for tandem duplicated genes of *SabZIP* involved in salt response. Based on GFF (General Feature Format) annotation files, tandem duplicated genes of *SabZIP* were identified in analysis on the basis of the following criteria: the distance between two adjacent *SabZIP* genes should be less than 1 Mb [18]. Among *SabZIP* genes in *S. australis*, a total of four pairs of tandem duplicated genes (*Sau08107* and
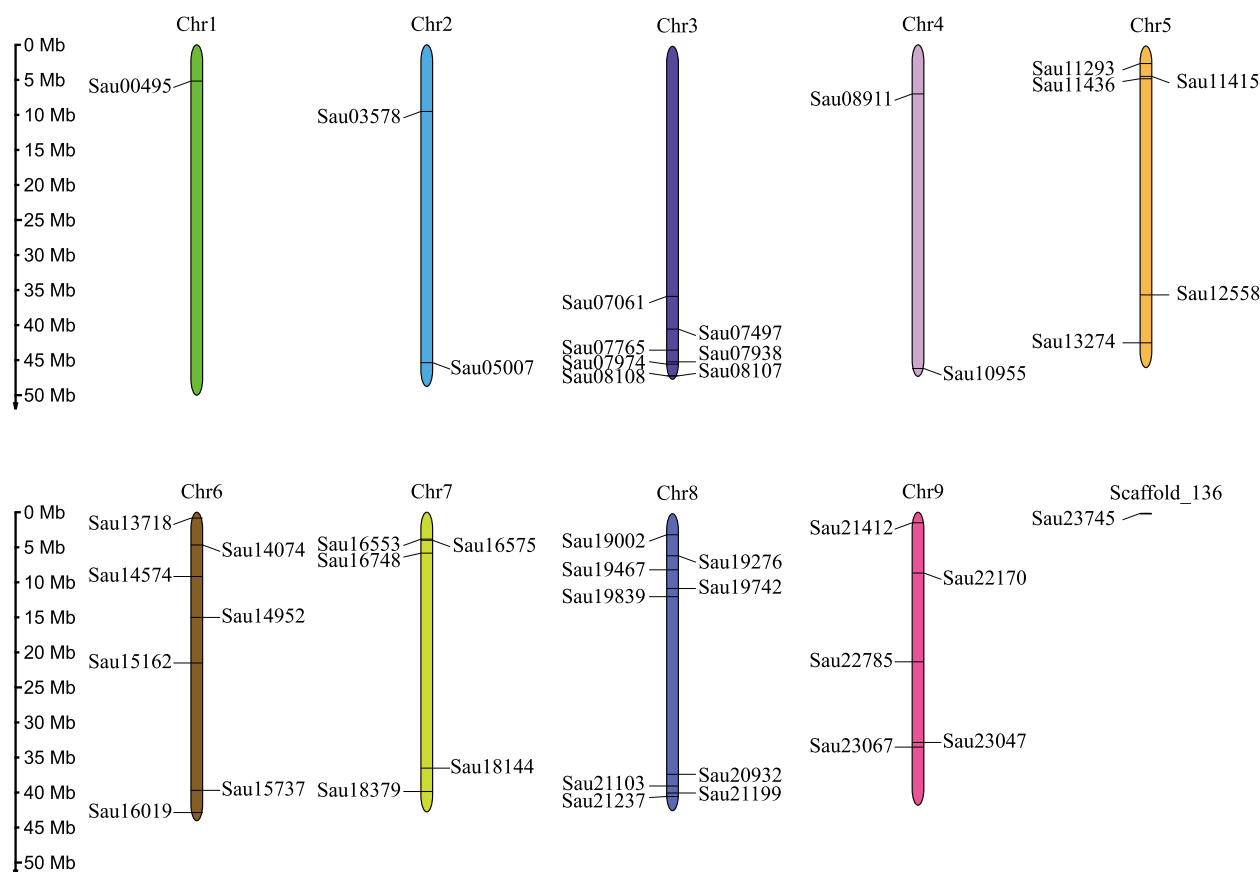
Qu *et al. BMC Plant Biology*   (2024) 24:816

Page 3 of 17

Fig. 1 Chromosome distribution of *SabZIP* genes. *S. australis* chromosome number is indicated at the base of each chromosome with different colors. The *SabZIP* genes are marked at the approximate position on the chromosomes

Sau08108, *Sau11415* and *Sau11436*, *Sau16553* and *Sau16575*, *Sau23047* and *Sau23067*) were observed, as illustrated in Fig. 1.

To examine the evolutionary relationships among the *bZIP* genes in these three species (*Arabidopsis thaliana*, *Beta vulgaris*, and *Oryza sativa*), syntenic analysis was performed (Fig. 2). A total of 32, 41, and 22 orthologous gene pairs of orthologous *SabZIP* genes were identified between *S. australis* and *A. thaliana*, *S. australis* and *B. vulgaris*, and *S. australis* and *O. sativa*, respectively (Fig. 2). In contrast, 19 collinear gene pairs initially identified between *S. australis* and *A. thaliana* were also found in the comparison between *S. australis* and *B. vulgaris*. Similarly, 11 collinear gene pairs initially associated with *S. australis* and *A. thaliana* were also observed when comparing *S. australis* with *O. sativa*. Furthermore, all 10 collinear gene pairs initially detected between *S. australis* and *O. sativa* were likewise identified when comparing *S. australis* with *B. vulgaris* (Fig. 2). Additionally, it's worth noting that each of the following species: *S. australis*, *A. thaliana*, *B. vulgaris*, and *O. sativa* shared 9 common collinear gene pairs (Fig. 2).

Phylogeny, structural, and conserved motifs analysis of *SabZIP* genes

To investigate the evolutionary relationships among *SabZIP* genes, we constructed a neighbor-joining (NJ) phylogenetic tree based on the full-length protein sequences (Fig. 3). *SabZIP* genes were categorized into 12 subfamilies from *S. australis* (Fig. 3). The A subfamily containing eight *SabZIP* family members, was the most extensive clade. In contrast, subfamilies F and J were the smallest, each comprising only one member. Furthermore, subfamilies H, C, K, B, E, I, G, D, and S consisted of 2, 2, 2, 2, 2, 5, 4, 7, and 7 members, respectively.

The gene structure analysis of the 44 *SabZIP* genes in *S. australis* is illustrated in Fig. 4. Our observations revealed notable variability in the gene structure of *SabZIP* members, with exon numbers ranging from 1 to 13. Notably, members of the G subfamily, namely Sau10955, Sau14074, and Sau19276 (except Sau07938), displayed a maximum of 13 exons, a distinctive feature distinguishing them from members of other subfamilies, where exon numbers ranged from 1 to 12. By contrast, the *Sau23745* of B subfamily contained 11 exons, but the other member
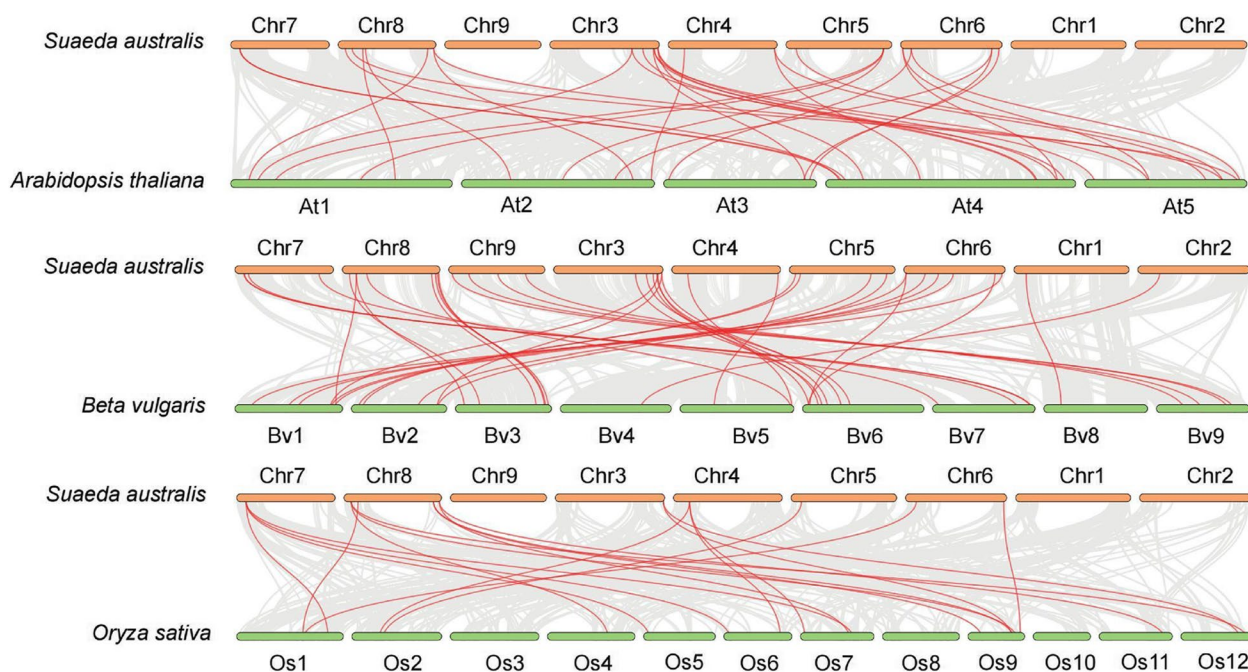
Qu *et al. BMC Plant Biology*   (2024) 24:816

Page 4 of 17

Fig. 2 Synteny analysis of *SabZIP* genes between *S. australis* and three plant species. The collinear blocks between *S. australis* and other three plant genomes are shown as the gray lines in the background, while the syntenic *SabZIP* gene pairs are highlighted with red lines

Sau21199 contained only two exons. Additionally, some *SabZIP* members within the same group exhibited similar gene structures. For instance, the exon numbers of H subfamily and S members were both 1 and lacked introns. All of C, K, and E subfamily members had 6, 4, and 4 exons, respectively. These results suggested that the structural features of *SabZIP* genes exhibit noticeable variations, even when considering members in the same gene subfamily.

A total of ten different motifs were identified in *SabZIP* gene family of *S. australis* (Fig. 4). All of *SabZIP* genes contained a bZIP domain (PF00170) represented by motif 1. Motif 7 and motif 8 were specific to the A subfamily of SabZIP family. Moreover, motif 2, motif 3, motif 4, and motif 6 occurred only in D subfamily. Each member belonging to S subfamily and H subfamily exhibited a shared pattern of two motifs (motif 1 and motif 10) within their gene structures. Motif 5 was shared only by two subfamilies (E and I). This collective evidence provided support for the notion that members in the same subfamily exhibit identical conserved motifs.

Estimation of nonsynonymous (Ka) and synonymous (Ks) substitution rates and Ka/Ks values

To investigate the selection pressures acting on *SabZIP* genes following duplication during their evolutionary history, we computed the nonsynonymous (Ka) to synonymous (Ks) substitutions for each paralogous pair,

as presented in Table 1. A total of four pairs of tandem duplications in *S. australis* were identified. The Ka/Ks ratio spanned from 0.7221 (*Sau23047* and *Sau23067*) to 1.0019 (*Sau23047* and *Sau23067*) with an average ratio of 0.8925. The Ka/Ks ratios of three paralogous *SabZIP* gene pairs (*Sau08107* and *Sau08108*, *Sau11415* and *Sau11436*, and *Sau23047* and *Sau23067*) were less than 1, indicating that these genes are subject to purifying selection. Conversely, the Ka/Ks value of (*Sau16553* and *Sau16575*) was slightly greater than 1, suggesting positive selection following duplication. Collectively, these results imply that the majority of these gene pairs have been subjected to purifying selection pressure, and the duplication events may contribute significantly to the expansion of the SabZIP family in *S. australis*.

Promoter region analysis of *SabZIP* genes

To discover cis-acting elements associated with mechanisms pertaining to the response to salt stress, we analyzed the promoter sequences of *S. australis* *SabZIP* genes. In *S. australis*, the cis-acting elements in promoters' regions of majority of *SabZIP* genes (more than 35 members) were mainly associated with anaerobic induction, transcription start, and light responsiveness (Fig. 5 and Table 2). In contrast, we also identified several cis-elements (RY-element, WUN-motif, TATC-box, HD-Zip 3, MBSI, ABRE, A-box, AACA_motif), which were present in a minority of members (less than 6
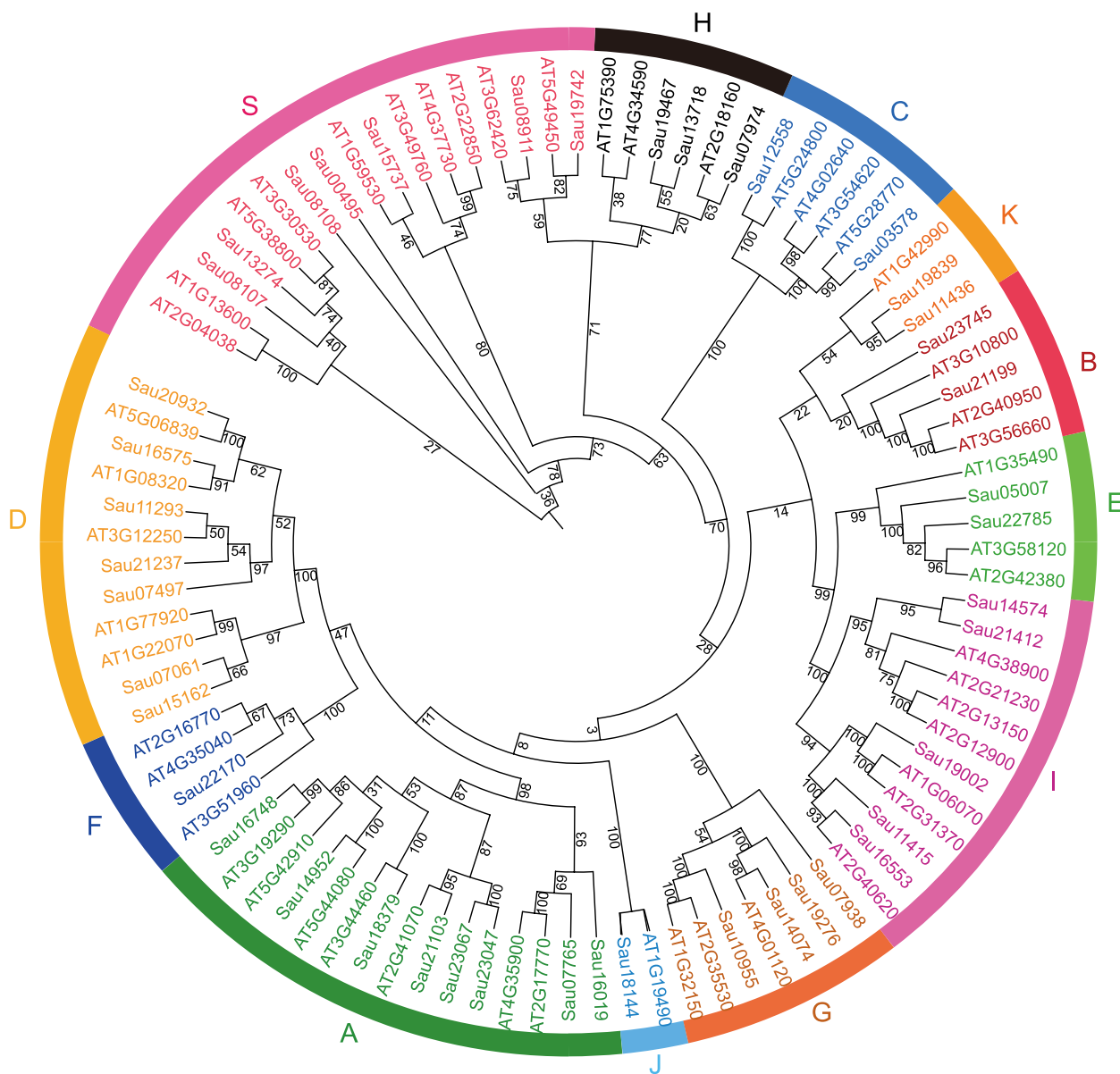
Qu *et al. BMC Plant Biology*   (2024) 24:816

Page 5 of 17

Fig. 3 Phylogenetic analysis of SabZIP proteins in *S. australis*. A neighbor-joining (NJ) tree was constructed using 44 SabZIP sequences. The tree further clustered into 12 subfamilies, which are shown in different colors

members) (Table 2). Phytohormone response elements, including abscisic acid, auxin, gibberellin, and MeJA, were also widely observed. Moreover, *SabZIP* members were also related to low-temperature responsiveness, circadian control, flavonoid biosynthetic genes regulation, drought-inducibility, seed-specific regulation, and stress responsiveness, suggesting their role in responding to various stresses and plant growth. These results offer valuable insights into the regulatory roles of *SabZIP* gene family during both stress responses and plant development.

Expression profiles of *SabZIP* genes under different salt concentrations

RNA-seq was performed on the Illumina HiSeqTM2000 system. The leaves under two salt treatment levels (ST1 and ST2) were used for transcriptomic expression profiles. In total, more than 27 million raw reads were obtained from each samples. After quality evaluation and filtration, the number of clean reads ranged from 27,179,940 to 30,399,735 with an average of 28,486,258 and the average value of Q30 was 95.82%, indicating that the clean reads were of high quality.
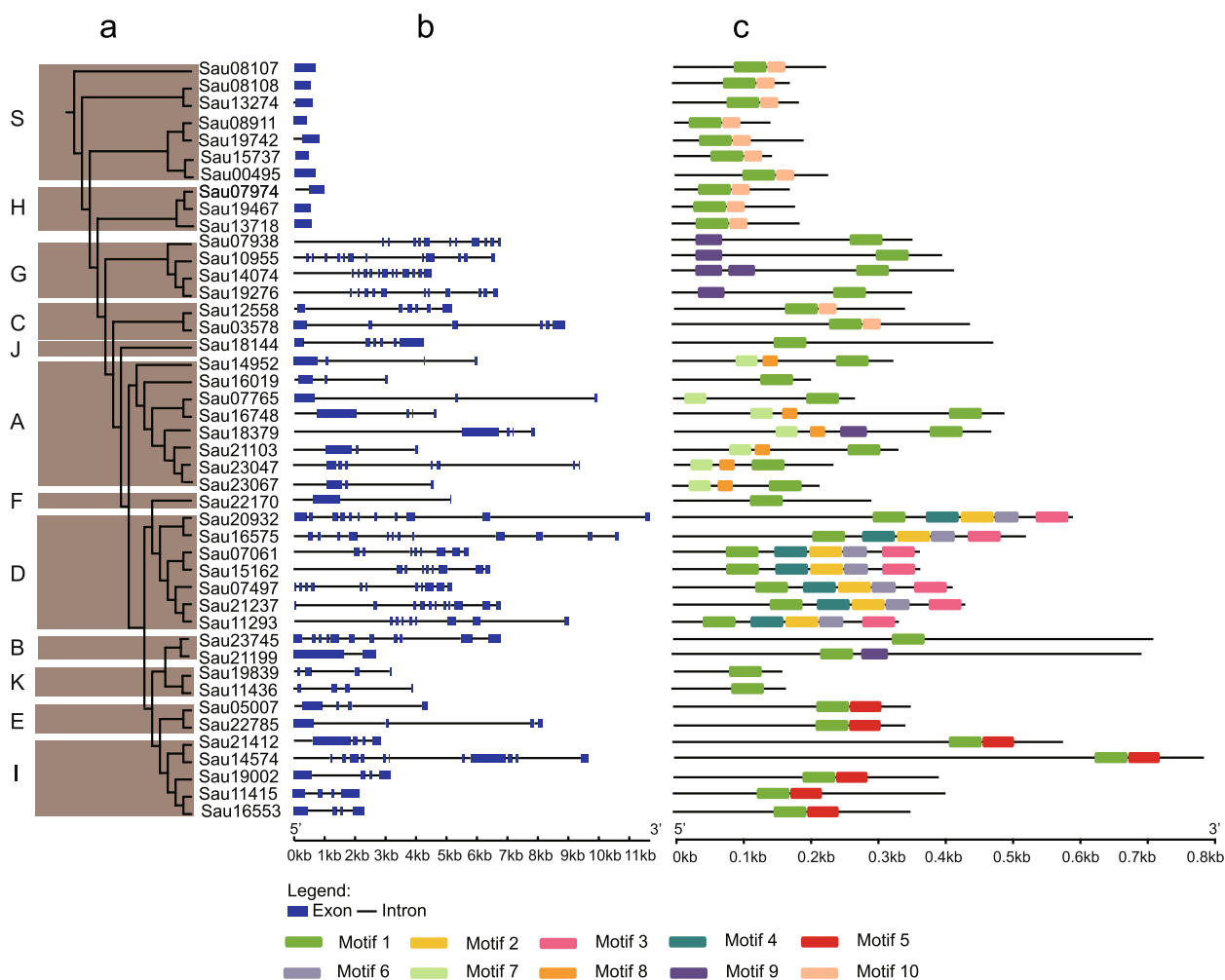
Qu *et al. BMC Plant Biology*   (2024) 24:816

Page 6 of 17

Fig. 4 The phylogenetic relationship, gene structure, and motif compositions of SabZIP proteins. **A** The phylogenetic relationships of bZIP proteins based on the NJ method. The various colors characterize the 12 subfamilies. **B** Gene structure of the *SabZIP* genes family was generated on the basis of the gene Structure Display Server. Exons (blue rectangles) and introns (black lines) are marked along with their sequence length. **C** Motif in SabZIP proteins were predicted by MEME. The conserved motifs are represented by different colored boxes

Table 1 Analysis of tandem duplication events of *SabZIP* gene pairs in *Suaeda australis*

Tandem duplicated genes	Ka	Ks	Ka/Ks	Purifying selection
Sau08107 and *Sau08108*	0.6874	0.7340	0.9365	Yes
Sau11415 and *Sau11436*	0.9783	1.0754	0.9096	Yes
Sau16553 and *Sau16575*	1.0004	0.9986	1.0019	No
Sau23047 and *Sau23067*	0.3744	0.5186	0.7221	Yes

After alignment with the *S. australis* genome sequence, more than 95% of the clean reads were mapped to the genome and paired-end reads were aligned to 24,371 *S. australis* annotated gene models. A pairwise comparison between ST1 and ST2 samples identified 2,434 DEGs. Among them, 1,568 and 866 genes were respectively up-regulated and down-regulated in ST2 compared to ST1. GO and KEGG enrichment analysis revealed that the 2,434 DEGs were significantly enriched in some primary biological pathways, such as response to reactive oxygen species, response to hypoxia, regulation of cytokine production, photosynthesis, biosynthesis of nucleotide sugars, starch and sucrose metabolism, which were closely related to salt response-regulating signaling pathways (Fig. 6).

To investigate the potential functions of *SabZIP* genes among *S. australis* under salt stress, we conducted RNA-seq analysis to investigate expression patterns of 44 *SabZIP* genes. We used FPKM values to build a heatmap (Fig.S1). Of 44 *SabZIP* genes, 35 were expressed

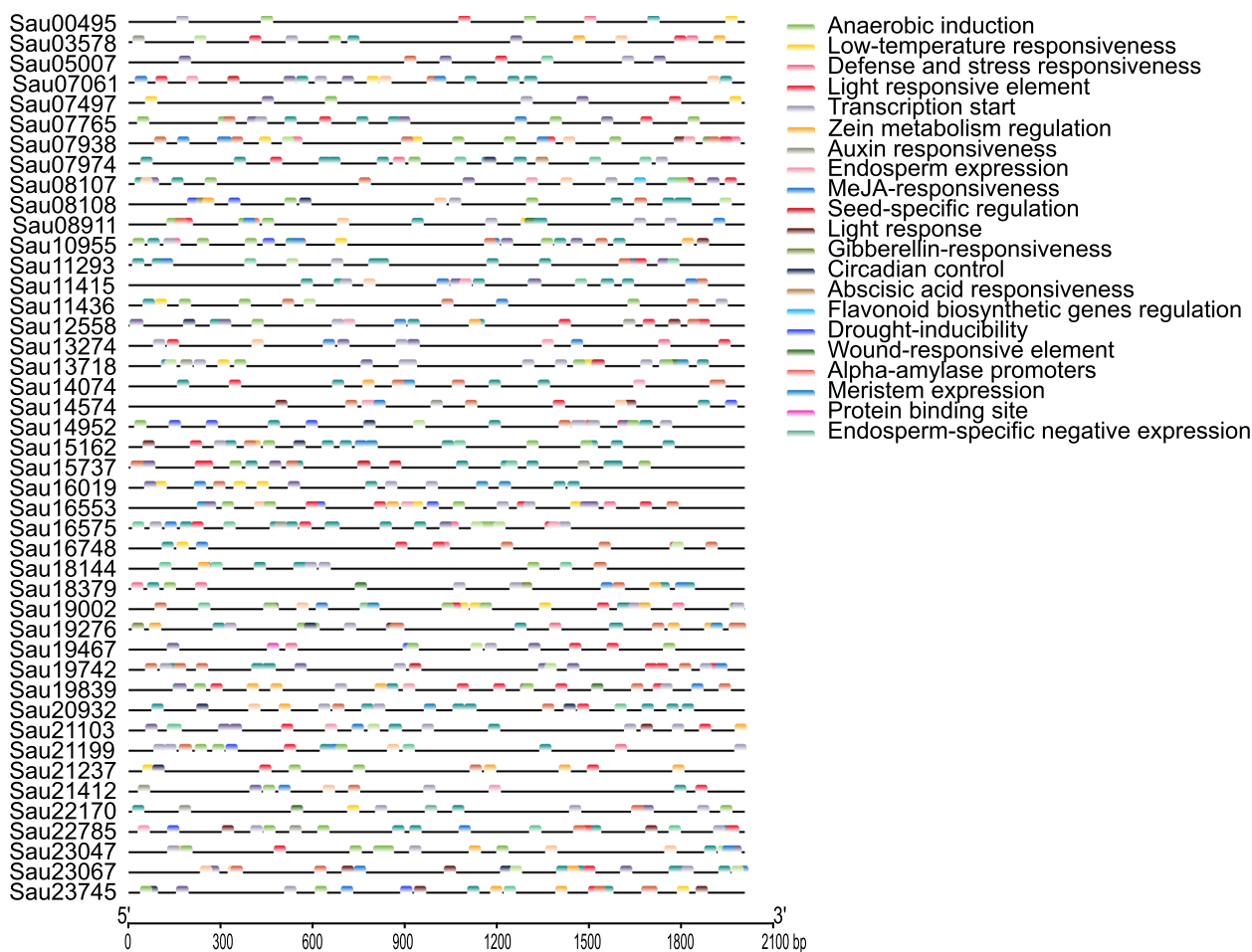Qu *et al. BMC Plant Biology*   (2024) 24:816

Page 7 of 17

Fig. 5 Cis-acting components of *SabZIP* genes in *Suaeda australis*. All promoter sequences (2000 bp) were analyzed. The *SabZIP* genes are shown on the left. Scale bar at the base indicates length of promoter sequence. The functions of cis-acting element can be found in Table 2

in ST1 samples and 39 were expressed in ST2 samples (FPKM > 0). Among different samples, *SabZIP* genes showed differences in expression patterns (Fig.S1). For instance, *Sau08911, Sau11415, Sau08107, Sau19276*, and *Sau16575* showed higher expression levels under higher salt concentration stress (ST2) than ST1 leaves. These results indicated that *SabZIP* genes may play a significant role in the salt tolerance of *S. australis*. Further, we found that the expression levels of subfamily S members (*Sau08107, Sau19742, Sau08108, Sau00495, Sau15737, Sau13274*) except for *Sau08911*, were lower than the other 11 subfamily members. However, the S subfamily *Sau08107* gene was highly expressed among two salt treatments of *S. australis* leaves. Furthermore, the majority of gene pairs undergoing tandem duplications exhibited distinct expression patterns. For example, *Sau11436* was strongly expressed in ST2 leaves, but *Sau11415* was weakly expressed in them (Fig. 7).

In addition, a total of six *SabZIP* genes, namely, S subfamily *SabZIP09* (*Sau08107*) and *SabZIP11* (*Sau08911*) genes; I subfamily *SabZIP14* (*Sau11415*) gene; D subfamily *SabZIP26* (*Sau16575*) gene; G subfamily *SabZIP31* (*Sau19276*) gene; and A subfamily *SabZIP36* (*Sau21103*) gene, were chosen for qRT-PCR analysis (three replicates for each gene). In general, the relative expression levels of selected genes were in agreement with FPKM values obtained from RNA-seq (Fig. 7), verifying the reliability of our transcriptomic expression profiles.

Effect of overexpression of selected *SabZIP* genes under different salt concentrations
To examine the subcellular localization of above six proteins (SabZIP09, SabZIP11, SabZIP14, SabZIP26, SabZIP31, and SabZIP36), vectors expressing each of above selected genes fused to GFP were constructed and used for a transient expression assay in *N. benthamiana*

Qu *et al. BMC Plant Biology*   (2024) 24:816

Page 8 of 17

Table 2 Cis-element and corresponding functions of *SabZIP* genes in *Suaeda australis*

| Cis-element	Function	Members
ARE	Cis-acting regulatory element essential for the anaerobic induction	44
TATA-box	Core promoter element around -30 of transcription start	39
G-Box	Cis-acting regulatory element involved in light responsiveness	35
TGACG-motif	Cis-acting regulatory element involved in the MeJA-responsiveness	30
LTR	Cis-acting element involved in low-temperature responsiveness	26
O2-site	Cis-acting regulatory element involved in zein metabolism regulation	20
TC-rich repeats	Cis-acting element involved in defense and stress responsiveness	17
GCN4_motif	Cis-regulatory element involved in endosperm expression	15
AE-box	Part of a module for light response	10
Circadian	Cis-acting regulatory element involved in circadian control	10
AuxRR-core	Cis-acting regulatory element involved in auxin responsiveness	9
MBS	MYB binding site involved in drought-inducibility	9
CAT-box	Cs-acting regulatory element related to meristem expression	8
RY-element	Cis-acting regulatory element involved in seed-specific regulation	5
WUN-motif	Wound-responsive element	5
TATC-box	Cis-acting element involved in gibberellin-responsiveness	4
HD-Zip 3	Protein binding site	4
MBSI	MYB binding site involved in flavonoid biosynthetic genes regulation	3
ABRE	Cis-acting element involved in the abscisic acid responsiveness	1
A-box	Sequence conserved in alpha-amylase promoters	1
AACA_motif	Involved in endosperm-specific negative expression	1
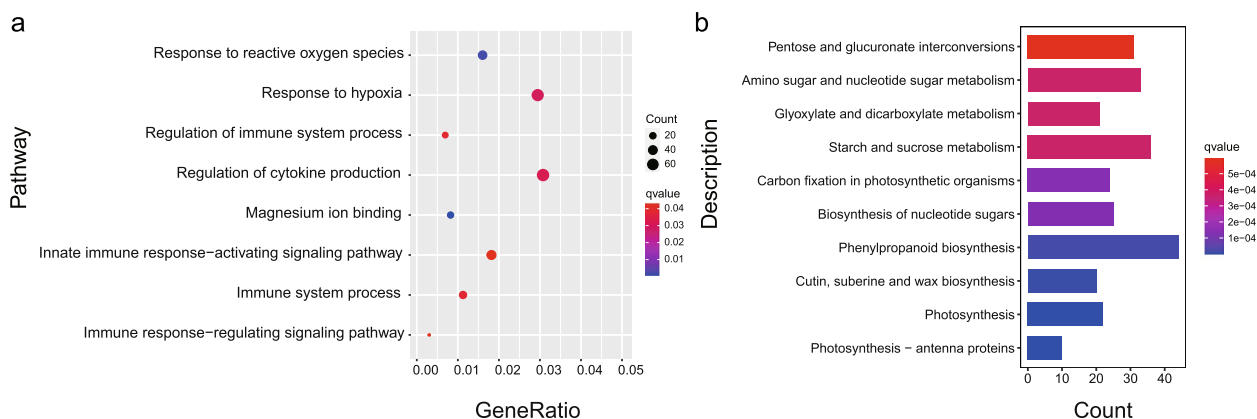
Fig. 6 GO (**a**) and KEGG (**b**) enrichment of 2,434 DEGs in ST1 and ST2 samples (ST2_vs_ST1)

leaf cells. All six SabZIP-GFP fusion proteins exclusively co-localized with H2B-mCherry in the nuclei (Fig. 8), suggesting that all six SabZIPs are nuclear proteins, consistent with their potential function as transcriptional regulators. Among six SabZIP proteins, SabZIP14, SabZIP26, and SabZIP36 showed the higher Percent Identity (>60% based on BLASTP with 1e-5 E-value) to known bZIP family proteins in tobacco, indicating potential functional conservation. To further investigate the mechanism by which SabZIPs regulate the downstream salt response-regulating genes at the transcriptional level, the expression of six stress responsive genes under the three independent transient overexpression lines (*SabZIP14*, *SabZIP26*, and *SabZIP36*) were measured by qRT-PCR (Fig. 9). In tobacco, *VRN1* and *PRE6*, *ATG8B* and *ATG8E*, *DGAT1* and *CAT1* could been regulated by transcription factor RF2b (orthologous gene of SabZIP14), TGA9 (SabZIP26), and ABI 5 (SabZIP36), respectively. The results showed that after salt treatment for 24 h, the expression levels of *VRN1*, *PRE6*, *ATG8B*,
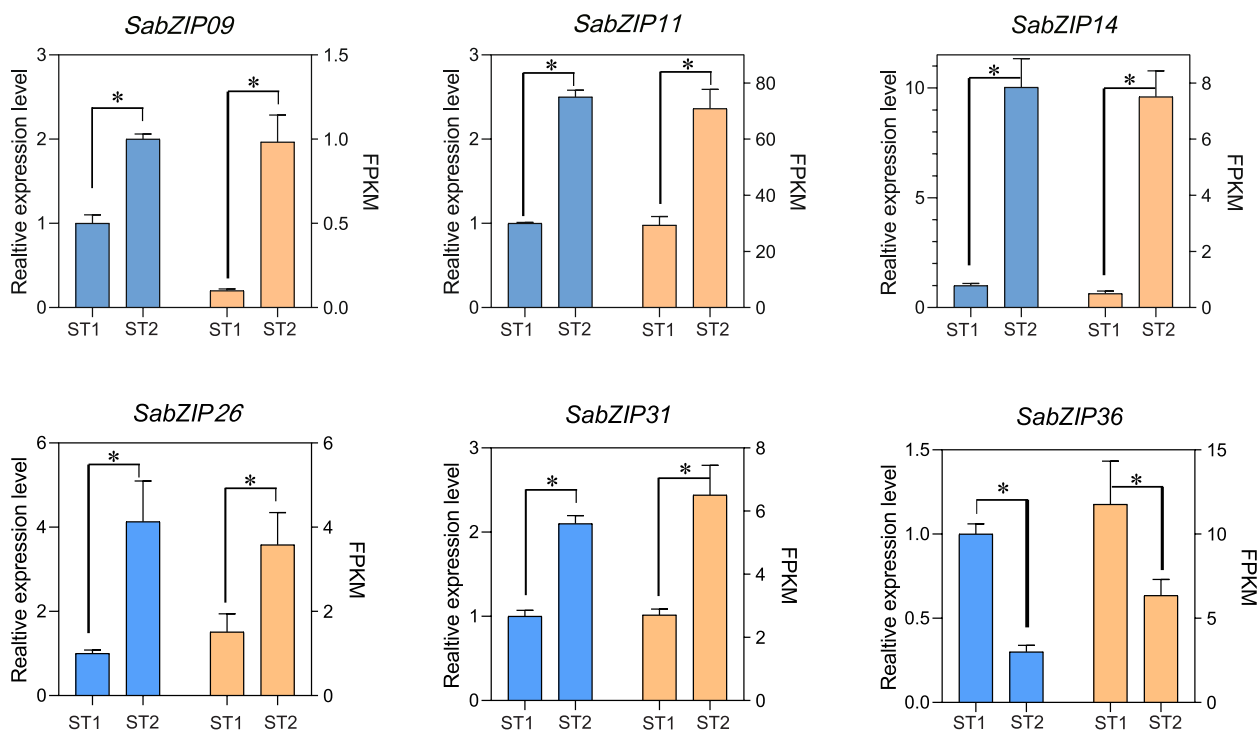
Qu *et al. BMC Plant Biology*   (2024) 24:816

Page 9 of 17

Fig. 7 Comparisons of expression levels of six *SabZIP* genes obtained by qRT-PCR analysis among ST1 and ST2 leaves of *Suaeda australis*. The left Y-axis indicates the relative expression level, right Y-axis indicates the FPKM, and the X-axis represents different samples after salt stress treatment taken for expression analysis; the mean ± standard error measurement (SEM) value with three replications ($n = 3$) is displayed. * indicates $p < 0.05$

ATG8E, *DGAT1*, and *CAT1* in the experimental group were significantly induced compared with the WT *N. benthamiana*. Interestingly, the expression of *PRE6* was only greatly decreased in the *SabZIP14*-overexpressing transient expressed line compared with the WT, whereas the transcript levels of other above five genes were significantly increased in transgenic lines. These results suggested that SabZIPs may enhance the resistance to salt stress by effectively activating the transcription of the downstream stress-related gene.

SabZIPs bind the promoter of downstream salt stress-related genes and activate their transcription

To explore whether SabZIP14, SabZIP26, SabZIP36 directly activate the expression of *VRN1* and *PRE6*,*ATG8B* and *ATG8E*, *DGAT1* and *CAT1*,respectively in *N. benthamiana*, yeast one-hybrid (Y1H) assays were carried out (Fig. 10). The results showed that GAD-SabZIP14 fusion protein, instead of GAD (GAL1 transcriptional activation domain, AD), respectively activated the LacZ reporter gene driven by the *VRN1* and *PRE6* promoter (Fig. 10a and b), indicating that SabZIP14 can bind to *VRN1* and *PRE6* promoter directly. In addition, the interaction of SabZIP26 or SabZIP36 with the promoter of *ATG8B* and *ATG8E* or *DGAT1* and *CAT1* in vitro were also confirmed by Y1H assays (Fig. 10c-f).

Subsequently, the transient expression assays were then performed using the dual-luciferase reporter system in *N. benthamiana* leaves. The results demonstrated that a strong LUC signal could be observed only in the leaves co-expressing 35S:SabZIP14 and *proPRE6-LUC*, 35S:SabZIP14 and *proVRN1-LUC*, 35S:SabZIP26 and *proATG8B-LUC*, 35S:SabZIP26 and *proATG8E-LUC*, 35S:SabZIP36 and *proDGAT1-LUC*, 35S:SabZIP36 and *proCAT1-LUC* (Fig. 11). The results indicated that SabZIP14, SabZIP26, SabZIP36 proteins could directly bind to the promoter region of *VRN1* and *PRE6*, *ATG8B* and *ATG8E*, *DGAT1* and *CAT1,* respectively to activate genes expression.

Discussion

bZIP transcription factors represent a prominent protein family in flowering plants engaged in stress responses, pathogen defence, light signaling, flower development, and seed maturation [13]. In this study, a genome-wide identification of the bZIP protein family was carried out in *S. australis*. The 44 identified bZIP proteins in *S. australis* were categorized into 12 distinct subfamilies, which correspond to the classification and identification results in *A. thaliana* [10]. Upon comparing the subfamily composition, we found that seven, two, five, and one SabZIP members in subfamilies S, C, I, and F were less
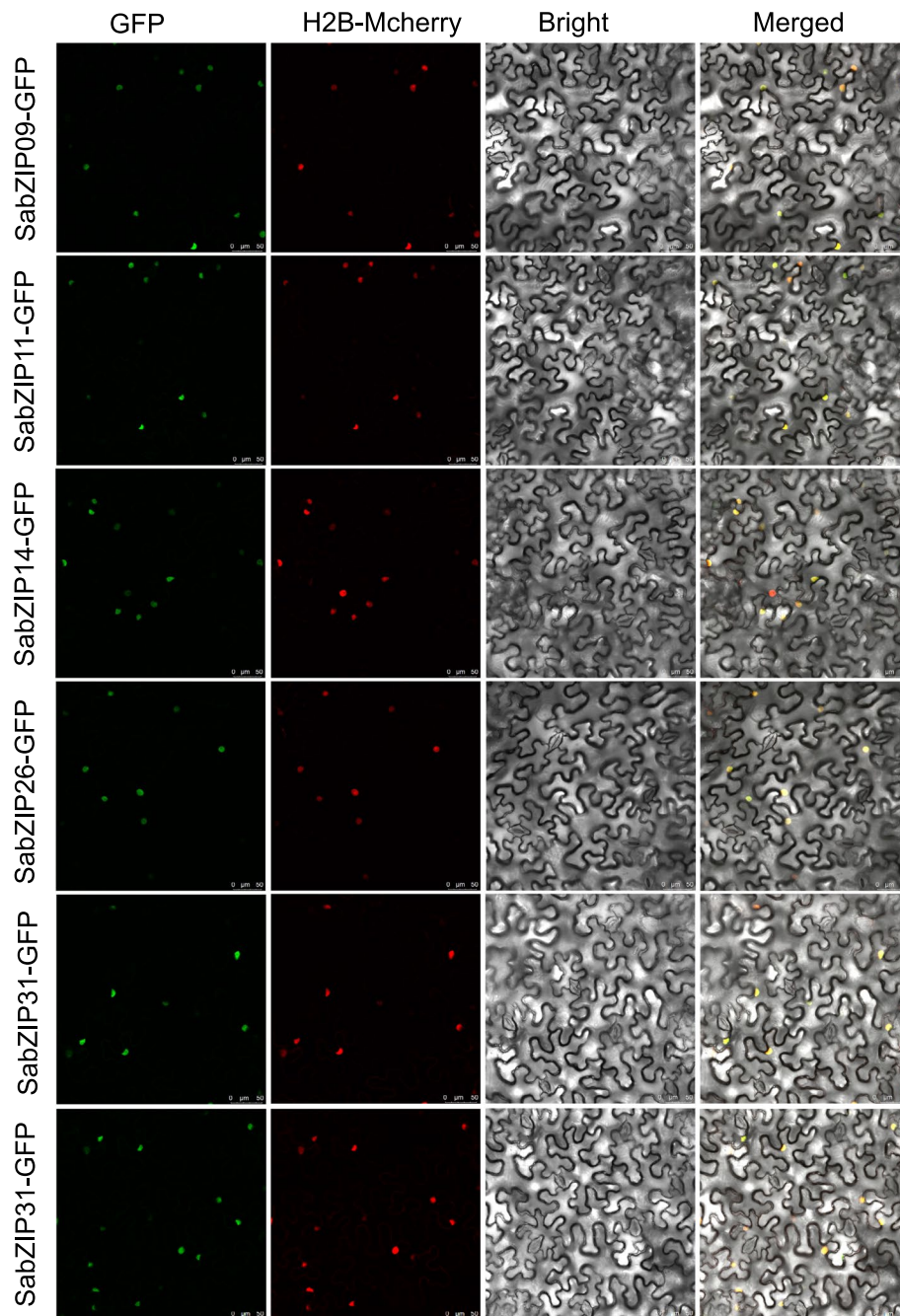
Qu *et al. BMC Plant Biology*   (2024) 24:816

Page 10 of 17

Fig. 8 Transient expression and subcellular localization of SabZIP09, SabZIP11, SabZIP14, SabZIP26, SabZIP31, and SabZIP36. The colocalization of SabZIP09-GFP, SabZIP11-GFP, SabZIP14-GFP, SabZIP26-GFP, SabZIP31-GFP, and SabZIP36-GFP, and nuclei was determined by the GFP signal and H2B-mCherry histone. GFP was used as a negative control. Scale bars, 10 μm

than ten, four, seven, and three in *A. thaliana*, respectively (Fig. 3). In contrast, subfamily A and D exhibited a higher count of members, with eight and seven SabZIP members compared to seven and five in *A. thaliana*, respectively (Fig. 3). It is worth noting that previous studies have documented the identification of *bZIP* genes in

numerous other plant species, such as 92 members in *Oryza sativa* [19], 125 members in *Zea mays* [20], 114 members in *Malus domestica* [21], and 86 members in poplar [22]. Similar to the *S. australis* family, the number of bZIP family in *Ziziphus jujuba* (45 bZIPs) and *Prunus mume* (49 bZIPs) show the relatively low level
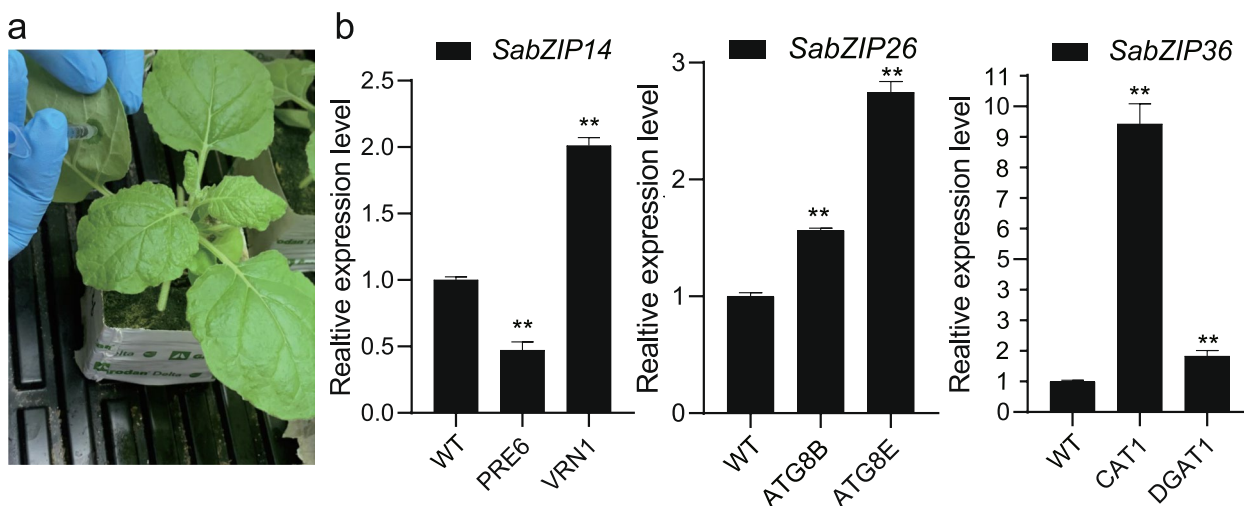
Fig. 9 Expression levels of *VRN1*, *PRE6*, *ATG8B*, *ATG8E*, *DGAT1*, and *CAT1* in the WT *N. benthamiana* and transient *SabZIPs* (*SabZIP14*, *SabZIP26*, and *SabZIP36*) overexpression lines as indicated. **$P < 0.01$

[23, 24], indicating the contraction of bZIP family during evolution. Furthermore, the assembled genome size of *S. australis* (437.17 Mb) was notably larger than that of *A. thaliana* (119.67 Mb) [25], indicating that there was no substantial correlation between genome size and the quantity of members. In a word, comparison of the *bZIP* genes number among various plants showed that the number of various species are also different.

Except for minority of subfamilies (S and H), the gene structures of *SabZIP* members exhibited visible variations, even in the same gene subfamily, particularly in terms of exon length and quantity (Fig. 4). Similar findings have been documented in cucumber [26] and *Cyclocarya paliurus* [27]. An analysis of motifs (Fig. 5) revealed the presence of 10 motifs in *S. australis*, designated as motif 1 through motif 10. Besides, motif compositions remained consistent within the same subfamily but exhibited variations among different subfamilies, indicating that subfamily-specific motifs may influence the functional divergence of *SabZIP* genes. These findings were consistent with previous study of *Carthamus tinctorius* [28] and *Glycyrrhiza uralensis* [29]. The diversifcation of subfamily-specific motifs provide ideas for investigating the function of bZIPs, and the diversifcation of functions enables plants to enhance their salt tolerance to adapt to the environment. Subfamily-specific motifs can lead to differences in the regulatory and binding properties of bZIP transcription factors, thereby influencing gene expression patterns under stress conditions. In *Arabidopsis*, most members belonging to group A contained subfamily-specific motif participate in ABA biological pathway and regulate plant responses to salt stress [30]. In peanut, group B bZIP proteins have a transmembrane

domain and a specific domain motif at the C-terminus, also are important to the salt stress response via endoplasmic reticulum stress signaling [31]. Therefore, the *SabZIP* genes in group A and B could have similar functions to *Arabidopsis and* peanut. Moreover, the analysis of the promoter region revealed that a majority of the cis-element components in *SabZIP* genes were associated with temperature responsiveness, circadian control, flavonoid biosynthetic genes regulation, drought-inducibility, seed-specific regulation, and stress responsiveness (Fig. 5).

Based on the expression profiles analysis, it was evident that genes in the same subfamily exhibited diverse expression patterns among two salt treatment samples, but small amounts of subfamily genes (*Sau08107*, *Sau19742*, *Sau08108*, *Sau00495*, *Sau15737*, and *Sau13274*) showed the similar expression profiles. The study suggested that genes in the same subfamily displayed distinct and varied expression patterns throughout the evolutionary process. In addition, these results could be attributed to the intrinsic requirement for paralogous genes of the same origin to prevent functional redundancy while generating subfunctions and novel functions [32]. As a typical halophyte, *S. australis* possesses a special structure with succulent leaves, which may effectively store water, reduce the concentration of salt ions in leaf cells, maintain the osmotic balance of leaf cells, and heavily contribute to salt-stress adaptability [33]. In our study, five *bZIP* DEGs containing *Sau08107*, *Sau08911*, *Sau11415*, *Sau16575*, and *Sau1927*6 showed higher expression levels in ST2 leaves than ST1. Among them, *Sau08107* and *Sau08911* belonging to group S, which could be directly activated via the ABA-dependent pathway, and form
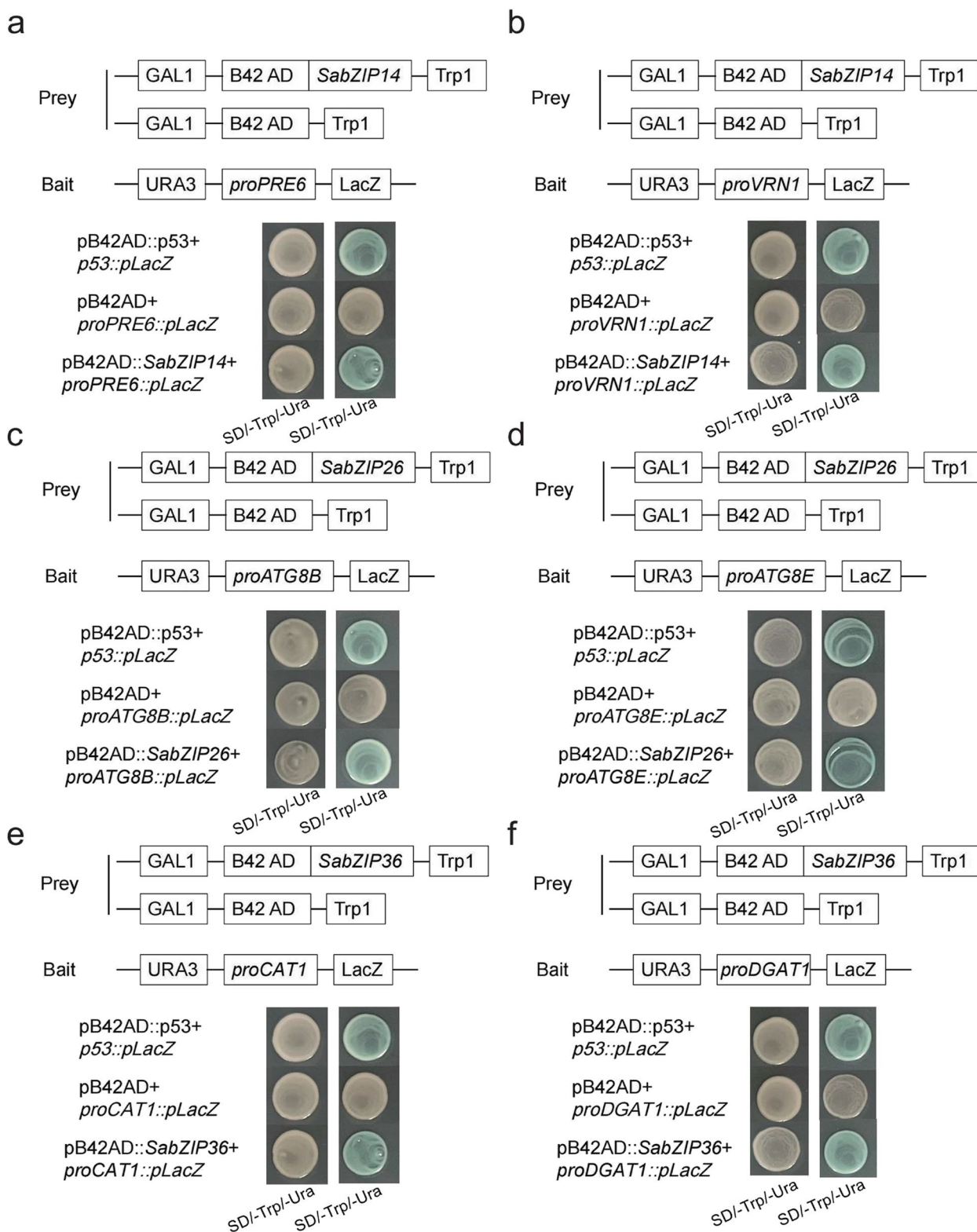
Fig. 10 Yeast onehybrid analysis, using pB42AD-SabZIP14 as the prey, *ProVRN1-pLacZ* and *ProPRE6-pLacZ* as the baits, respectively; pB42AD-SabZIP26 as the prey, *ProATG8B-pLacZ* and *ProATG8E-pLacZ* as the baits, respectively; pB42AD-SabZIP36 as the prey, *ProDGAT1-pLacZ* and *ProCAT1-pLacZ* as the baits, respectively; pB42AD-p53 and *p53-pLacZ* as the positive controls
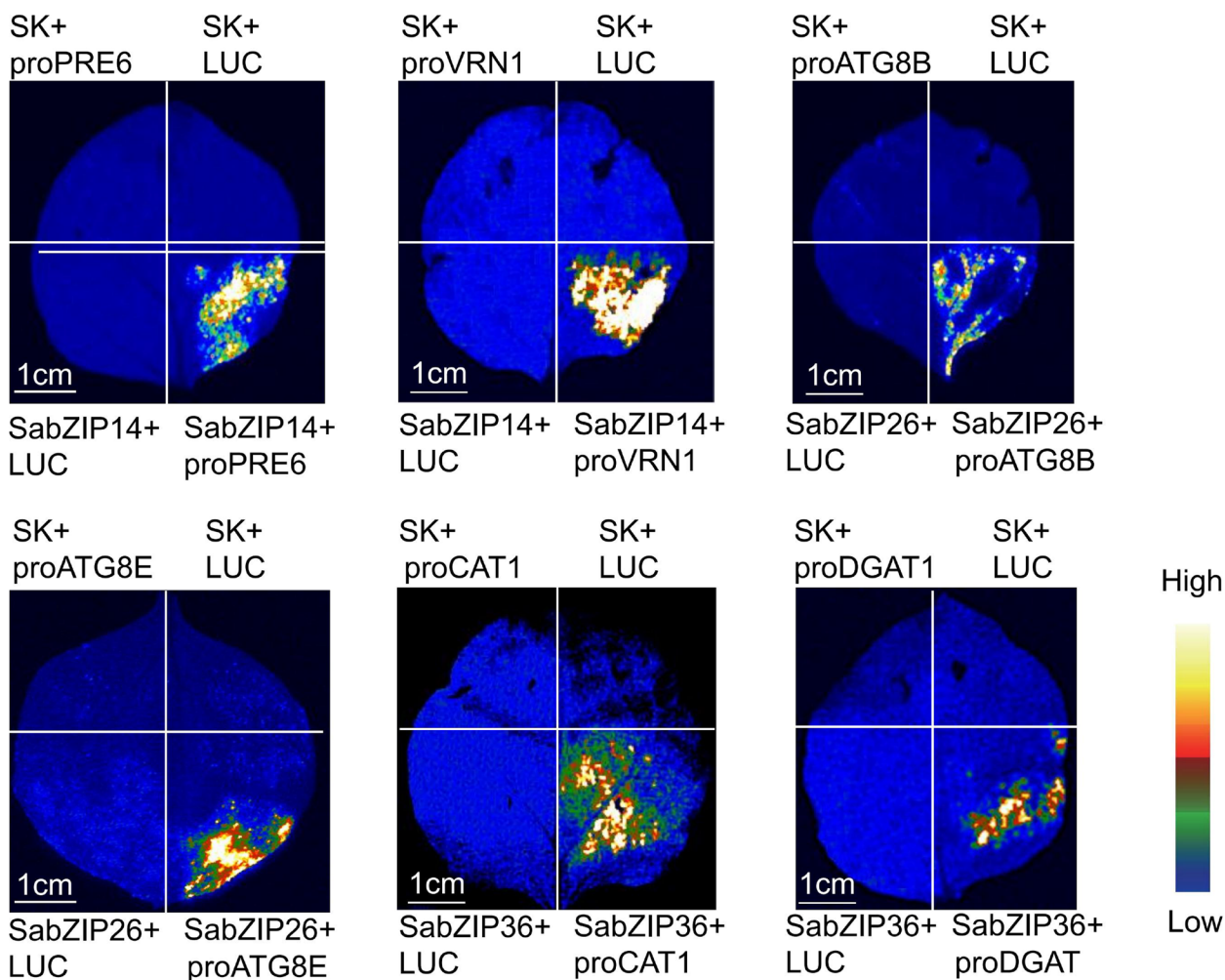
Qu *et al. BMC Plant Biology*   (2024) 24:816

Page 13 of 17

Fig. 11 The luciferase signal was detected in *N. benthamiana* leaves

heterodimeric complexes with other members of the bZIP family under the salt stress in rice [34]; group I gene (*Sau11415*) is involved in cell cycle regulation and salt stress response [10]; *Sau16575* belongs to group D, which can regulate the growth and development and decrease the sensitivity to salt stress in plants [35]; group G *bZIP* gene (*Sau19276*), has been demonstrated as an inhibitor of salt stress tolerance in tomato [36].

The molecular mechanism of plant stress resistance has been a hot topic in biological research. Previous studies have reported that bZIPs can participate in abiotic stress responses, but no studies have been reported in *S. australis*. In this study, we aimed to fully understand the function of *bZIP* genes in *S. australis*. We found all six differentially expressed SabZIPs are nuclear proteins and were positively activate the *VRN1* [37], *PRE6* [38], *ATG8B* [39], *ATG8E* [40], *DGAT1* [41], and *CAT1* [42] involved in the salt stress response. We speculate that these *SabZIPs* may have the same expression pattern

as their significantly related transcription factors. This research provides information for research on *SabZIPs* functions. In conclusion, our results demonstrated the significant roles of the *SabZIP* gene family in salt stress and plant growth.

Conclusions

Australis is a typical halophyte distributed in subtropical and tropical coastal areas. Research has mainly focused on increasing yield, quality, and stress tolerance in *S. australis*. The *bZIP* gene family is significantly associated with plant growth, development, and the tolerance to salt stress. In this study, we identified 44 members of *bZIP* gene families in *S. australis*. Expression patterns analyses clearly discovered the role of several *SabZIPs* including *Sau08107*, *Sau08911*, *Sau11415*, *Sau16575*, and *Sau19276*, which showed higher expression levels in higher salt concentration than low concentration and obviously response to salt

stress. Moreover, SabZIP14, SabZIP26, and SabZIP36 proteins could respectively bind to the promoter region of *VRN1* and *PRE6*, *ATG8B* and *ATG8E*, *DGAT1* and *CAT1* and activate their expressions. These results improve our understanding of the role of *bZIPs* in developmental processes and in salt stress and provide a theoretical basis for further studies aimed at exploring the regulation of salt stress responses in *S. australis*.

Materials and methods

Plant materials, cDNA synthesis, and transcriptome sequencing

In the present study, the plants of *S. australis* were grown in Dinghai District, Zhoushan City, Zhejiang Province, China (E122°11′, N30°02′) and then transplanted to Fishery College, Zhejiang Ocean University. Voucher specimens were identified by Yinquan Qu, and deposited in Molecular Ecology Lab of Zhejiang Ocean University (Voucher code: 2022–1-ZS). In addition, we treated plants with salt treatment (ST) with two levels (ST1: the salt concentration of the soil was 10 g/kg; ST2: 18 g/kg) [43]. The leaves were sampled in reproductive development stage (24 October 2022) from *S. australis* individuals with one year old. The leaves were immediately collected and rapidly frozen in liquid nitrogen, followed by storage at − 80 °C. Each leaf sample consisted of three distinct biological replicates, each of which consisted of tissues from three individual plants. Total RNA extraction was performed employing the E.Z.N.A Plant RNA Isolation Kit (OMEGA, USA). Concentration and purity of RNAs were assessed using the NanoDrop spectrophotometer 2000C (Thermo Fisher Scientific, Waltham, MA, USA), while confirmation of RNA integrity was achieved through 1.0% agarose gel electrophoresis. The RNAs with OD_{260}/OD_{280} valus within the range of 1.8–2.0 were subsequently subjected to reverse transcription into cDNA using PrimeScript™ RT reagent kit with gDNA Eraser (TaKaRa, China), following the manufacturer's protocols. The resulting cDNAs were subsequently diluted at a 1:10 ratio with RNase-free water and stored at -20 °C for future qRT-PCR analyses. The cDNA libraries were constructed using the NEBNext® UltraTM RNA Library Prep Kit following the manufacturer's instruction. All cDNA libraries were sequenced using an Illumina HiSeqTM2000 system, generating reads with a length of 2×100 bp. Any sequences of low quality (defined by bases with Q-scores < 10%), sequences below 50 bp in length, primer sequences, and adapter sequences were rigorously filtered and excluded from the initial raw data by fastp [44].

Identification of *SabZIP* genes in *S. australis*

The whole protein sequence of *S. australis* was obtained from the Genome Warehouse (GWH) at the National Genomics Data Center, Beijing Institute of Genomics (https://ngdc.cncb.ac.cn/gwh, accessed on 10 July 2023). To identify bZIP proteins within *S. australis*, we initiated our search using *Arabidopsis* bZIP protein sequences as our query [10]. We initiated a comprehensive search for potential bZIP proteins using the local alignment search tool (BLASTP) [45] with a stringent E-value threshold of less than 1e-5. Following this preliminary screening, we acquired the HMM (hidden Markov model) profile corresponding to the Pfam bZIP domain (PF00107) from the Pfam database (http://pfam.xfam.org/, accessed on 10 July 2023). Subsequently, we employed this HMM profile to perform a search against the *S. australis* protein dataset using HMMER v3.3.2 [46] with default parameters. The acquired sequences underwent a rigorous filtration process based on two specific criteria: (1) incomplete sequences were eliminated if their lengths fell below that of the conserved motif (33 bp). (2) sequences containing more than 10 consecutive 'N' bases were excluded from further analysis. This culling process was employed to ensure data quality and conformity to research standards.

Chromosome location and synteny analysis of *SabZIP* genes

The precise chromosome locations of *S. australis bZIP* genes were determined using the MapGene2Chrom wb v2 tool (http://mg2c.iask.in/mg2c_v2.0/, accessed on 10 July 2023) on the basis of genome annotation obtained from the GWH database. The CDS sequences and genome feature file of *Arabidopsis thaliana* (genome assembly TAIR10.1) [47], *Beta vulgaris* (genome assembly EL10.2) [48], and *Oryza sativa* (genome assembly IRGSP-1.0) [49] were downloaded from https://www.ncbi.nlm.nih.gov/datasets/genome/GCF_000001735.4/, https://www.ncbi.nlm.nih.gov/datasets/genome/GCF_026745355.1/, and https://www.ncbi.nlm.nih.gov/datasets/genome/GCF_001433935.1/, respectively. To explore the synteny relationship of homologous *bZIP* genes in *S. australis* and above three species (*A. thaliana*, *B. vulgaris*, and *O. sativa*), we employed the Multiple Collinearity Scan toolkit (MCScanX) [50].

Prediction of *cis*-regulatory elements of promoter region

The 2000 bp sequences located upstream of *SabZIP* genes were obtained from the whole-genome sequence. To predict a variety of cis-acting regulatory elements, these sequences were subjected to analysis using the default parameters of the PlantCARE promoter analysis tool, accessible at http://bioinformatics.psb.ugent.be/

Qu *et al. BMC Plant Biology*   (2024) 24:816

Page 15 of 17

webtools/plantcare/html/ as of 10 July 2023. This analysis aimed to predict various cis-acting regulatory elements [51].

Estimation of Ka/Ks values

MCScanX was used to perform gene duplication analyses for *S. australis* genome [50]. BLASTP software was applied to search for candidate homologous gene pairs (E-value < 1e-5) from the *S. australis* genome [45]. To identify syntenic chains, the candidate homologous gene pairs were analyzed using MCScanX with default parameters. MCScanX was used to further distinguish among segmental and tandem duplication events in bZIP gene family [50]. Subsequently, the Ka and Ks substitution rates were computed through the utilization of the KaKs_Calculator toolkit based on verified duplicated gene pairs of the bZIP family [52].

Expression analysis of selected *SabZIP* genes

After quality control and adapter trimming of the RNA-seq reads, the paired-end short reads were aligned to *S. australis* genome using HiSAT2 with its default parameters. Subsequently, the calculation of the expected number of FPKM fragments mapped was performed employing the StringTie program [53] with default parameters. Moreover, the DESeq2 R package [54] was applied to identify the differentially expressed genes (DEGs). In multiple analyses, the threshold of the p-value was calculated by the false discovery rate (FDR). If the FDR was less than 0.05, and the absolute value of $\log_2$(fold change) was more than 1, the gene expression differences were considered to be significant. In addition, the Gene Ontology (GO) functional annotation and Kyoto Encyclopedia of Genes and Genomes (KEGG) pathway analysis were performed using the clusterProfiler R package [55].

Six *SabZIP* DEGs (*Sau08107*, *Sau08911*, *Sau11415*, *Sau16575*, *Sau19276*, and *Sau21103*) related to salt tolerant were screened for qRT-PCR analysis. The online software Primer3Plus (https://www.primer3plus.com/index.html) was used to design primers, and the primers were synthesized by Beijing Qinke Xinye Biotechnology Ltd. (Beijing, China) (Supplementary Table S2). qRT-PCR was conducted using SYBR qPCR Master MIX (Vazyme) [56] and performed on StepOnePlus (Applied Biosystem, USA) [57]. *18S ribosomal RNA* as an internal control was carried out. The methods for calculating relative gene expression were introduced by previous study [58].

Vector construction and subcellular localization

The full-length coding sequence (CDS) of *Sau08107*, *Sau08911*, *Sau11415*, *Sau16575*, *Sau19276*, and *Sau21103* genes harboring Kpn I and BamH I restriction sites were inserted into pCAMBIA2300-35S-eGFP via in-fusion cloning. Above six recombinant pCAMBIA2300-35S-SabZIP-eGFP vectors were further introduced into the GV3101 *Agrobacterium tumefaciens* strain for subcellular localization and transient expression in tobacco (*Nicotiana benthamiana*). We cloned the nuclear-located *AtH2B* gene from *A. thaliana* [59]. Then we constructed recombinant pCAMBIA2300-35S-AtH2B-Mcherry plasmid as a positive control, and was also transformed into *Agrobacterium* GV3101. The engineered *Agrobacterium* of 35S::SabZIP-eGFP and positive control (35S::AtH2B-Mcherry) were cultured with 30 ml LB medium at 28℃ for 16 h, respectively. Centrifuging the culture at 6000 ×g for 5 min, and then re-suspending the pellet in infiltration buffer (containing sterile deionized water, 10 mM MES, 150 uM AS, and 10 mM MgCl$_2$) with an OD600 of 1.0. Finally, we mixed the interest suspensions with equal volume proportion of positive control culture, respectively. The mixed suspension cultures were placed for 3 hours in the darkness. Tobaccos were grown in the greenhouse with a light/dark photoperiod of 16/8 h at 25℃. The leaves were infiltrated with infiltration buffer containing recombinant strains and were stored in a growth chamber during 60 h. All images were visualized by Leica TCS SP8X DLS laser confocal microscope. Meanwhile, RNA extraction and cDNA synthesis for qRT-PCR were performed on the infiltrated tobacco leaves after 24 hours of salt treatment.

Yeast one-hybrid assay

For Y1H system, the CDS of three *SabZIPs* (*SabZIP14*, *SabZIP26*, and *SabZIP36*) were individually were fused to the GAL1 AD in the pB42AD vectors to generate the prey vectors (pB42AD-SabZIP14, pB42AD-SabZIP26, and pB42AD-SabZIP36). The promoter fragments of *VRN1*, *PRE6*, *ATG8B*, *ATG8E*, *DGAT1*, and *CAT1* were individually constructed into pLacZi vectors to construct the baits. pB42AD-SabZIP14, pB42AD-SabZIP26, and pB42AD-SabZIP36 vectors were individually transformed into the EGY48 yeast strains. After selecting the transformants on SD/-Trp plates, the NcoI-cut bait vectors were respectively introduced into the EGY48 yeast strains harbouring pB42AD–SabZIP14, pB42AD-SabZIP26, and pB42AD-SabZIP36. Positively co-transformed cells were screened on SD/-Trp/-Ura medium and cultured at 30 °C for 3 days. The resultant transformants were tested for β-galactosidase activity on selective media (SD/-Trp/-Ura/BU salt/X-gal). A positive (pB42AD-p53 + *p53-LacZi*) control was processed in the same manner.

Qu *et al. BMC Plant Biology*   (2024) 24:816

Page 16 of 17

Dual-luciferase assay

Dual-luciferase assays were conducted as the method outlined previously [60]. The promoter regions of *VRN1*, *PRE6*, *ATG8B*, *ATG8E*, *DGAT1*, and *CAT1* were each cloned into pGreenII-0800-LUC reporter vectors, resulting in constructs such as *proVRN1*-LUC, *proPRE6*-LUC, *proATG8B*-LUC, *proATG8E*-LUC, *proDGAT1*-LUC, and *proCAT1*-LUC. The coding sequences (CDS) of *SabZIP14*, *SabZIP26*, and *SabZIP36* were individually inserted into the pGreenII 62-SK vector under the control of the CaMV35S promoter, generating the effector constructs (*35S::SabZIP14*, *35S::SabZIP26*, and *35S::SabZIP36*). After co-infiltrating the effector and reporter plasmids into *N. benthamiana* leaves via Agrobacterium for 48 h, the leaves were treated with 1mM D-Luciferin potassium salt and subjected to fluorescence imaging using a living imaging system.

Supplementary Information

The online version contains supplementary material available at https://doi.org/10.1186/s12870-024-05535-1.

> Supplementary Material 1.
>
> Supplementary Material 2.
>
> Supplementary Material 3.

Availability of data and materials
A total of 6 transcriptome raw datasets produced by HiSeqTM2000 system were deposited in the Genome Sequence Archive (SRA) database (https://ngdc.cncb.ac.cn/gsa/browse/CRA011892) under the accession number CRA011892. The genome sequences of *S. australis* was from the Genome Warehouse in National Genomics Data Center Beijing Institute of Genomics (https://ngdc.cncb.ac.cn/gwh/Assembly/64339/show#, accession number GWHDOOL00000000).

Declarations

Ethics approval and consent to participate
The materials of *S. australis* in this experiment were collected from *S. australis* germplasm resources bank (E122°11′, N30°02′) of the Fishery College, Zhejiang Ocean University, located in Molecular Ecology Laboratory of Zhejiang Ocean University, Zhoushan, Zhejiang Province, China. The collection of plant material complies with institutional guidelines and legislation.

Consent for publication
Not applicable.

Competing interests
The authors declare no competing interests.

References

1. Villa JA, Bernal B. Carbon sequestration in wetlands, from science to practice: An overview of the biogeochemical process, measurement methods, and policy framework. Ecol Eng. 2018;114:115–28.
2. Xi Y, Peng S, Ciais P, Chen Y. Future impacts of climate change on inland Ramsar wetlands. Nat Clim Change. 2021;11:45–51.
3. Sapkota Y, White JR. Carbon offset market methodologies applicable for coastal wetland restoration and conservation in the United States: a review. Sci Total Environ. 2020;701:134497.
4. Guo JM, Chen YY, Lu PZ, Liu M, Sun P, Zhang ZM. Roles of endophytic bacteria in *Suaeda salsa* grown in coastal wetlands: plant growth characteristics and salt tolerance mechanisms. Environ Pollut. 2021;287:117641.
5. Herbert ER, Boon P, Burgin AJ, Neubauer SC, Franklin RB, Ardon M, Hopfensperger KN, Lamers LPM, Gell P. A global perspective on wetland salinization: ecological consequences of a growing threat to freshwater wetlands. Ecosphere. 2015;6:206.
6. Ou YX, Sheng Y, Hu XJ, Leng DJ, Huang JF, Hu ZY, Bai LQ, Deng ZX, Kang QG, Wu YY. *Nonomuraea nitratireducens* sp. nov., a new actinobacterium isolated from *Suaeda australis* Moq. rhizosphere. Int J Syst Evol Micr. 2020;70(9):5026–31.
7. Kim H, Park GN, Jung BK, Yoon WJ, Chang KS. Antibacterial activity of *Suaeda australis* in halophyte. Journal of the Korean Applied Science and Technology. 2016;33(2):278–85.
8. Huang XK, Huang XD, Bian MJ. Study on the flavonoids compounds of *Suaeda australis* contents and its antioxidant activity in vitro. J Anhui Agric Sci. 2010;38(3):1432–34, +1542. (in Chinese)
9. Alam MR, Tran TKA, Stein TJ, Rahman MM, Griffin AS, Yu RMK, MacFarlane GR. Accumulation and distribution of metal(loid)s in the halophytic *saltmarsh shrub*, *Austral seablite*, *Suaeda australis* in New South Wales. Australia Mar Pollut Bull. 2021;169:112475.
10. Dröge-Laser W, Snoek BL, Snel B, Weiste C. The *Arabidopsis* bZIP transcription factor family-an update. Curr Opin Plant Biol. 2018;45:36–49.
11. Wang LF, Zhu JF, Li XM, Wang SM, Wu J. Salt and drought stress and ABA responses related to bZIP genes from *V. radiata* and *V. angularis*. Gene. 2018;651:152–60.
12. Joo H, Baek W, Lim CW, Lee SC. Post-translational modifications of bZIP transcription factors in abscisic acid signaling and drought responses. Curr Genomics. 2021;22(1):4–15.
13. Jakoby M, Weisshaar B, Dröge-Laser W, Vicente-Carbajosa J, Tiedemann J, Kroj T, Parcy F. bZIP transcription factors in *Arabidopsis*. Trends Plant Sci. 2002;7:106–11.
14. Mukherjee K, Choudhury AR, Gupta B, Gupta S, Sengupta DN. An ABRE-binding factor, OSBZ8, is highly expressed in salt tolerant cultivars than in salt sensitive cultivars of indica rice. BMC Plant Biol. 2006;6:18.
15. Lu G, Gao CX, Zheng XN, Han B. Identification of *OsbZIP72* as a positive regulator of ABA response and drought tolerance in rice. Planta. 2009;229:605–15.
16. Hossain MA, Cho JI, Han MH, Ahn CH, Jeon JS, An GH, Park PB. The ABRE-binding bZIP transcription factor OsABF2 is a positive regulator of abiotic stress and ABA signaling in rice. J Plant Physiol. 2010;167:1512–20.
17. Hossain MA, Lee YJ, Cho JI, Ahn CHH, Lee SK, Jeon JS, Kang H, Lee CH, An GH, Park PB. The bZIP transcription factor OsABF1 is an ABA responsive element binding factor that enhances abiotic stress signaling in rice. Plant Mol Biol. 2010;72:557–66.
18. Liu GE, Ventura M, Cellamare A, Chen L, Cheng Z, Zhu B, Eichler EE. Analysis of recent segmental duplications in the bovine genome. BMC Genom. 2009;10:1–16.
19. Guedes Corrêa LG, Riaño-Pachón DM, Guerra Schrago C, Vicentini dos Santos R, Mueller-Roeber B, Vincentz M. The role of bZIP transcription factors in

Qu *et al. BMC Plant Biology*   (2024) 24:816

Page 17 of 17

green plant evolution: adaptive features emerging from four founder genes. PloS One. 2008;3(8):e2944.

20. Wei KF, Chen J, Wang YM, Chen YH, Chen SX, Lin YN, Pan S, ZhongXJ, Xie DX. Genome-wide analysis of bZIP-encoding genes in maize. DNA Res. 2012;19(6):463–76.

21. Li YY, Meng D, Li MJ, Cheng LL. Genome-wide identification and expression analysis of the bZIP gene family in apple (*Malus domestica*). Tree Genet Genomes. 2016;12:82.

22. Zhao K, Chen S, Yao WJ, Cheng ZH, Zhou BR, Jiang TB. Genome-wide analysis and expression profile of the bZIP gene family in poplar. BMC Plant Biol. 2021;21:122.

23. Zhang Y, Gao WL, Li HT, Wang YK, Li DK, Xue CL, Liu ZG, Liu MJ, Zhao J. Genome-wide analysis of the bZIP gene family in Chinese jujube (*Ziziphus jujuba* Mill). BMC Genom. 2020;21:483.

24. Li P, Zheng TC, Li LL, Wang J, Cheng TR, Zhang QX. Genome-wide investigation of the bZIP transcription factor gene family in *Prunus mume*: Classification, evolution, expression profile and low-temperature stress responses. Hortic Plant J. 2022;8(2):230–42.

25. Sloan DB, Wu ZQ, Sharbrough J. Correction of persistent errors in *Arabidopsis* reference mitochondrial genomes. Plant Cell. 2018;30(3):525–7.

26. Baloglu MC, Eldem V, Hajyzadeh M, Unver T. Genome-wide analysis of the bZIP transcription factors in cucumber. PLoS ONE. 2014;9(4):e96014.

27. Tao YT, Chen LX, Jin J, Du ZK, Li JM. Genome-wide identification and analysis of *bZIP* gene family reveal their roles during development and drought stress in Wheel Wingnut (*Cyclocarya paliurus*). BMC Genom. 2022;23:743.

28. Li HY, Li LX, ShangGuan GD, Jia C, Deng SN, Noman M, Liu YL, Guo YX, Han L, Zhang XM, Dong YY, Ahmad N, Du LN, Li HY, Yang J. Genome-wide identification and expression analysis of bZIP gene family in *Carthamus tinctorius* L. Sci Rep. 2020;10(1):15521.

29. Han YX, Hou ZN, He QL, Zhang XM, Yan KJ, Han RL, Liang ZS. Genome-Wide characterization and expression analysis of *bZIP* gene family under abiotic stress in *Glycyrrhiza uralensis*. Front Genet. 2021;12:754237.

30. Finkelstein RR, Lynch TJ. The *Arabidopsis* abscisic acid response gene ABI5 encodes a basic leucine zipper transcription factor. Plant Cell. 2000;12(4):599–609.

31. Wang Z, Yan L, Wan L, Huai D, Kang Y, Shi L, Jiang H, Lei Y, Liao Y. Genome-wide systematic characterization of bZIP transcription factors and their expression profiles during seed development and in response to salt stress in peanut. BMC Genom. 2019;20:1–14.

32. Kong WL, Gong ZY, Zhong H, Zhang Y, Zhao GQ, Gautam M, Deng XX, Liu C, Zhang CH, Li YS. Expansion and evolutionary patterns of glycosyltransferase family 8 in gramineae crop genomes and their expression under salt and cold stresses in *Oryza sativa* ssp. japonica. Biomolecules. 2019;9(5):188.

33. Robinson SP, Downton WJS. Potassium, sodium and chloride ion concentrations in leaves and isolated chloroplasts of the halophyte *Suaeda australis* R. Br Funct Plant Bio. 1985;12(5):471–9.

34. Liu CT, Mao BG, Ou SJ, Wang W, Liu LC, Wu YB, Chu CC, Wang XP. OsbZIP71, a bZIP transcription factor, confers salinity and drought tolerance in rice. Plant Mol Biol. 2014;84:19–36.

35. Li B, Liu Y, Cui XY, Fu JD, Zhou YB, Zheng WJ, Lan JH, Jin LG, Chen M, Ma YZ, Xu ZS, Min DH. Genome-wide characterization and expression analysis of soybean TGA transcription factors identified a novel TGA gene involved in drought and salt tolerance. Front Plant Sci. 2019;10:549.

36. Pan YL, Hu X, Li CY, Xu X, Su CG, Li JH, Song HY, Zhang XG, Pan Y. SlbZIP38, a tomato bZIP family gene downregulated by abscisic acid, is a negative regulator of drought and salt stress tolerance. Genes. 2017;8(12):402.

37. Liu J, Yao YY, Xin MM, Peng HR, Ni ZF, Sun QX. Shaping polyploid wheat for success: Origins, domestication, and the genetic improvement of agronomic traits. J Integr Plant Biol. 2022;64(2):536–63.

38. Fan S, Jia Y, Wang R, Chen X, Liu W, Yu H. Multi-omics analysis the differences of VOCs terpenoid synthesis pathway in maintaining obligate mutualism between Ficus hirta Vahl and its pollinators. Front Plant Sci. 2022;13:1006291.

39. Wang P, Nolan TM, Yin Y, Bassham DC. Identification of transcription factors that regulate ATG8 expression and autophagy in *Arabidopsis*. Autophagy. 2020;16(1):123–39.

40. Magen S, Seybold H, Laloum D, Avin-Wittenberg T. Metabolism and autophagy in plants-a perfect match. FEBS Lett. 2022;596(17):2133–51.

41. Kong Y, Chen S, Yang Y, An C. ABA-insensitive (ABI) 4 and ABI5 synergistically regulate DGAT1 expression in *Arabidopsis* seedlings under stress. FEBS Lett. 2013;587(18):3076–82.

42. Collin A, Daszkowska-Golec A, Szarejko I. Updates on the role of ABSCISIC ACID INSENSITIVE 5 (ABI5) and ABSCISIC ACID-RESPONSIVE ELEMENT BINDING FACTORs (ABFs) in ABA signaling in different developmental stages in plants. Cells. 2021;10(8):1996.

43. Chen LH, Zhang H, Yao YT, Zhang C, Zheng JH, Zhang FG. Effects of *Suaeda salsa* covering on soil physicochemical properties in coastal beach. J Plant Resour & Environ. 2021;30(2):19–27.

44. Chen S, Zhou Y, Chen Y, Gu J. fastp: an ultra-fast all-in-one FASTQ preprocessor. Bioinformatics. 2018;34(17):i884–90.

45. Lavigne R, Seto D, Mahadevan P, Ackermann HW, Kropinski AM. Unifying classical and molecular taxonomic classification: analysis of the Podoviridae using BLASTP-based tools. Res Microbiol. 2008;159(5):406–14.

46. Prakash A, Jeffryes M, Bateman A, Finn RD. The HMMER web server for protein sequence similarity search. Curr Protoc Bioinformatics. 2017;60(1):3–15.

47. Naish M, Alonge M, Wlodzimierz P, Tock AJ, Abramson BW, Schmücker A, Henderson IR. The genetic and epigenetic landscape of the *Arabidopsis centromeres*. Science. 2021;374(6569):eabi7489.

48. McGrath JM, Funk A, Galewski P, Ou S, Townsend B, Davenport K, Dorn KM. A contiguous de novo genome assembly of sugar beet EL10 (*Beta vulgaris* L.). DNA Res. 2023;30(1):dsac033.

49. Kawahara Y, de la Bastide M, Hamilton JP, Kanamori H, McCombie WR, Ouyang S, Matsumoto T. Improvement of the *Oryza sativa* Nipponbare reference genome using next generation sequence and optical map data. Rice. 2013;6:1–10.

50. Wang YP, Tang HB, Debarry JD, Tan X, Li JP, Wang XY, Lee TH, Jin HZ, Guo H, Kissinger JC, Paterson AH. MCScanX: a toolkit for detection and evolutionary analysis of gene synteny and collinearity. Nucleic Acids Res. 2012;40(7):e49.

51. Lescot M, Déhais P, Thijs G, Marchal K, Moreau Y, Van de Peer Y, Rouzé P, Rombauts S. PlantCARE, a database of plant cis-acting regulatory elements and a portal to tools for in silico analysis of promoter sequences. Nucleic Acids Res. 2002;30(1):325–7.

52. Zhang Z. KaKs_Calculator 3.0: calculating selective pressure on coding and non-coding sequences. Genom Proteom Bioinf. 2022;20(3):536–40.

53. Pertea M, Kim D, Pertea GM, Leek JT, Salzberg SL. Transcript-level expression analysis of RNA-seq experiments with HISAT. StringTie and Ballgown Nat Protoc. 2016;11(9):1650–67.

54. Love MI, Huber W, Anders S. Moderated estimation of fold change and dispersion for RNA-seq data with DESeq2. Genome Biol. 2014;15:1–21.

55. Yu GC, Wang LG, Han YY, He QY. clusterProfiler: an R package for comparing biological themes among gene clusters. Omics: a j integrat biol. 2012;16(5):284–7.

56. Zheng HH, Zhang SJ, Cui JT, Zhang J, Wang LY, Liu F, Chen HY. Simultaneous detection of classical swine fever virus and porcine circovirus 3 by SYBR green I-based duplex real-time fluorescence quantitative PCR. Mol Cell Probe. 2020;50:101524.

57. Cao Y, Sivaganesan M, Kinzelman J, Blackwood AD, Noble RT, Haugland RA, Griffith JF, Weisberg SB. Effect of platform, reference material, and quantification model on enumeration of Enterococcus by quantitative PCR methods. Water Res. 2013;47(1):233–41.

58. Qu YQ, Chen XL, Mao X, Huang P, Fu XX. Transcriptome analysis reveals the role of GA$_3$ in regulating the asynchronism of floral bud differentiation and development in heterodichogamous *Cyclocarya paliurus* (Batal.) Iljinskaja. Int J Mol Sci. 2022;23(12):6763.

59. Jiang D, Borg M, Lorković ZJ, Montgomery SA, Osakabe A, Yelagandula R, Axelsson E, Berger F. The evolution and functional divergence of the histone H2B family in plants. PLoS Genet. 2020;16(7):e1008964.

60. Fan L, Wang Y, Xu L. A genome-wide association study uncovers a critical role of the *RsPAP2* gene in red-skinned *Raphanus sativus* L. Hortic Res. 2020;7(1):164.

Publisher's Note